FEBS Letters 589 (2015) 639–644

journal homepage: www.FEBSLetters.org

Structural insights into *Cn*-AMP1, a short disulfide-free multifunctional peptide from green coconut water

Mábio J. Santana [a], Aline L. de Oliveira [b], Luiz H.K. Queiroz Júnior [a], Santi M. Mandal [c], Carolina O. Matos [a], Renata de O. Dias [e], Octavio L. Franco [d,e,*], Luciano M. Lião [a,*]

[a] *Institute of Chemistry, Federal University of Goiás, Goiânia, GO, Brazil*
[b] *Institute of Chemistry, University of Brasília, Brasília, DF, Brazil*
[c] *Central Research Facility, Indian Institute of Technology Kharagpur, Kharagpur 721302, WB, India*
[d] *Centro de Analises Proteomicas e Bioquímicas, Pós-graduação em Ciências Genomicas e Biotecnologia, Brasília, DF, Brazil*
[e] *S-Inova, Programa de Pós-Graduação em Biotecnologia, Universidade Católica Dom Bosco, Campo Grande, MS, Brazil*

ARTICLE INFO

Article history:
Received 13 May 2014
Revised 16 January 2015
Accepted 22 January 2015
Available online 29 January 2015

Edited by Christian Griesinger

Keywords:
Promiscuous peptide
Antimicrobial
NMR structure
SDS micelles
Green coconut water
Cn-AMP1

ABSTRACT

Multifunctional and promiscuous antimicrobial peptides (AMPs) can be used as an efficient strategy to control pathogens. However, little is known about the structural properties of plant promiscuous AMPs without disulfide bonds. CD and NMR were used to elucidate the structure of the promiscuous peptide *Cn*-AMP1, a disulfide-free peptide isolated from green coconut water. Data here reported shows that peptide structure is transitory and could be different according to the micro-environment. In this regard, *Cn*-AMP1 showed a random coil in a water environment and an α-helical structure in the presence of SDS-d_{25} micelles. Moreover, deuterium exchange experiments showed that Gly4, Arg5 and Met9 residues are less accessible to solvent, suggesting that flexibility and cationic charges seem to be essential for *Cn*-AMP1 multiple activities.

1. Introduction

The increasing number of pathogens that are resistant to conventional antibiotics has resulted in a strong effort to develop novel antimicrobial agents, especially those with unusual mechanisms of action. Antimicrobial peptides (AMPs) can be used as an efficient strategy to control bacterial development since they have a broad spectrum of activity against pathogens, including bacteria, fungi and virus [1,2]. There are multiple possible ways in which a multifunctional peptide may lead to bacterial death, including peptide interaction with cellular membranes of phospholipids, thus causing disruption, or due to a peptide binding onto cytoplasmic components, causing a deleterious interference in their metabolism [2].

Furthermore, in addition to multiple functions, there are also a wide number of AMP sources including microorganisms, invertebrates, animals and plants [3–5]. In the case of plant tissues, AMPs have also been isolated from flowers, leaves, roots and seeds, among others [5–8]. Recently, three antimicrobial peptides were isolated from green coconut water (*Cn*-AMPs), in a series called *Cn*-AMP1 (SVAGRAQGM), *Cn*-AMP2 (TESYFVFSVGM) and *Cn*-AMP3 (YCSYTMEA) [9]. These three peptides showed deleterious activity against multiple Gram-positive and Gram-negative pathogenic bacteria, with *Cn*-AMP1 being more active against four bacterial strains including *Escherichia coli*, *Bacillus subtilis*, *Staphylococcus aureus* and *Pseudomonas aeruginosa*. Nevertheless, it is also known that AMPs are evolutionarily ancient molecules that could act as constituents of the innate immune system. Recently, it was demonstrated that a single plant AMP can achieve multiple functions, and this ability is known as peptide promiscuity [10]. In this context, *Cn*-AMP1 was also challenged against fungal pathogens and cancerous cells, showing clear activity. Interestingly, an extra in vitro immunostimulatory activity was exerted by *Cn*-AMP1, showing that coconut peptide was capable of up-regulating inflammatory-cytokine secretion by monocytes [11], suggesting multiple action mechanisms.

These features give the peptide *Cn*-AMP1 a promiscuous character, even not presenting disulfide bond connection [9,11]. However, little is known about structural properties in plant promiscuous AMPs without disulfide bonds. In this view this study was performed in order to shed some light on the functional–structural relations of

* Corresponding authors at: Universidade Católica de Brasília, Brasília, DF, Brazil (O.L. Franco). NMR Laboratory, Institute of Chemistry, Federal University of Goiás, Goiânia, GO 74001-970, Brazil (L.M. Lião).

E-mail addresses: ocfranco@gmail.com (O.L. Franco), lucianoliao@ufg.br (L.M. Lião).

http://dx.doi.org/10.1016/j.febslet.2015.01.029
0014-5793/

the promiscuous peptide *Cn*-AMP1, a promising disulfide-free plant peptide with reduced size and cationic and hydrophobic properties. The knowledge of NMR *Cn*-AMP1 tertiary structure should help toward a better understanding of the mode of action of plant promiscuous peptides, indicating intramolecular interactions that govern peptide structure under different conditions.

2. Materials and methods

2.1. Peptide synthesis and mass spectrometry

Cn-AMP1 was purchased from the company Peptide 2.0 Incorporated (USA) which synthesized the peptide with 95% of purity after TFA removal by stepwise solid-phase synthesis using the N-9-fluorenylmethyloxycarbonyl (Fmoc) strategy [12]. *Cn*-AMP1 was purified using reversed-phase HPLC, and molecular mass was confirmed and determined using MALDI–ToF MS/MS analysis (Autoflex, Bruker Daltonics, Billerica, MA). The purified peptide was dissolved in the smallest water volume that was mixed with an α-cyano-4-hydroxycinnamic acid saturated matrix solution (1:3, v:v), spotted onto a MALDI ToF target plate and dried at room temperature for 5 min. The α-cyano-4-hydroxycinnamic acid matrix solution was ready at 50 mM in H_2O:CAN:TFA (50:50:0.3, v:v:v). Peptide monoisotopic mass was acquired in the reflector mode with external calibration, using the Peptide Calibration Standard II for mass spectrometry (up to 4000 Da mass range, Bruker Daltonics, Billerica, MA).

2.2. Circular dichroism

Circular dichroism (CD) experiments were carried out using a Jasco 815 spectropolarimeter (JASCO International Co. Ltd.), coupled to a Peltier Jasco PTC-423L system for temperature control. In the experiments carried out in the presence of SDS micelles, 50 μM of peptide were added in solutions of 10, 20, 50 and 100 mM sodium dodecyl sulfate (SDS) in water. pH variation was also studied and samples were prepared to a final peptide concentration of 50 μM and 100 mM of SDS in phosphate buffer at pH 3.97 and buffer tris–HCl at pH 7.00. Spectra were collected and averaged over six scans in the spectral range of 190–260 nm, with 0.1 mm path length quartz cells at 25 °C. A 0.2 nm step resolution, 50 nm min^{-1} speed, 1 s response time, and 1 nm bandwidth, were used. Following baseline correction, the observed ellipticity, θ (mdegree) was converted to the molar mean residue ellipticity [θ] (degree cm^2 $dmol^{-1}$).

2.3. NMR sample preparation

Initially, 500 μL of a solution containing deionized H_2O and HCl, adjusted to pH 3.97, was prepared and divided into two aliquots of 250 μL. In the first fraction 17.60 mg of SDS-d_{25} with 98% purity was added. In the second fraction 0.47 mg of *Cn*-AMP1 peptide was added. Finally, the two aliquots were mixed and 50 μL of D_2O:TMSP-d_4 solution (99:1 v/v) was added. The final solution volume was ~550 μL, corresponding to a concentration of 1.0 mM of the peptide and 100 mM of the SDS-d_{25}. In order to evaluate the 3D structure of *Cn*-AMP1 in the absence of surfactant agent another samples with pH at 3.97 were prepared under the same conditions listed above, without SDS-d_{25}.

2.4. NMR data acquisition

All NMR data were acquired at 25 °C using a Bruker Avance III 500 NMR spectrometer operated at 11.75 T (^{1}H resonance frequency 500.13 MHz), equipped with a 5 mm TBI probe (^{1}H, ^{13}C and XBB). The 2D ^{1}H–^{1}H TOCSY and NOESY experiments were recorded with presaturation as appropriate and using time proportional phase increment (States TPPI/States) for quadrature detection in F1. The mixing times were set to 80 ms for TOCSY (4K × 256, 184 scans) and 200 ms for NOESY experiments (4K × 512, 104 scans). The TOCSY and NOESY data were processed using the program NMRPipe package [13], and converted to the format NMRView [14].

2.5. Molecular modeling

The calculation of structures was carried out using the program XPLOR-NIH [15] by simulated annealing (SA) method [16]. Interactions were classified into short (2.8 Å), medium (3.4 Å) and long (5.0 Å) range [17]. The structure calculation started with an extended model, with 18 000 steps at high temperature, and 9000 steps of cooling. The ensemble of 20 lower energy structures (from 200 calculated structures) was chosen to represent the peptide solution 3D structure. The structural analysis was performed using PROCHECK [18] and the structures were visualized using PyMOL software [19]. The hydrogen bonds were identified using PyMOL software [19], with the distances and angles calculated using Protein Interactions Calculator (PIC) web server [35].

2.6. Hydrogen–deuterium exchange

For the determination of the peptide kinetics in SDS micelles, hydrogen–deuterium (H/D) exchange was monitored by NMR spectroscopy. In H/D exchange experiments, the 1 mM of peptide sample incorporated in 100 mM of SDS-d_{25} micelles were lyophilized. The lyophilized material was then dissolved in H_2O/D_2O (60:40) at pH 3.97 and soon after a TOCSY spectrum was acquired as described previously. Subsequently, a series of TOCSY spectra were acquired for 732 min.

3. Results and discussion

In the present work, the structure of plant disulfide-bond-free multifunctional peptide *Cn*-AMP1 was studied by CD and NMR in the presence and absence of SDS micelles.

The far-UV CD spectrum of *Cn*-AMP1 in aqueous solution shows a typical spectrum of a peptide in a random coil conformation, with a negative minimum at 190 nm (Fig. 1A). When interacting with SDS micelles, the peptide acquired an α-helical fold, characterized by two minimums at 208 and 222 nm (Fig. 1B). The maximum α-helical content results occurred in the presence of 100 mM of SDS. The influence of pH variation was also evaluated, and CD spectra were obtained at pH 3.97 and 7.00 in the presence of 100 mM of SDS. Fig. 1C shows that little variation of *Cn*-AMP1 helical content was observed when both pHs were compared, but at pH 3.97 the peptide has a maximum conformation. Then, beyond aqueous solution, 100 mM of SDS and pH 3.97 was the chosen condition to determine the *Cn*-AMP1 structure by NMR.

Both TOCSY spectra, in the presence and absence of SDS, showed well-resolved signals, making it possible to identify the chemical shifts of ^{1}H backbone and side chains of all amino acid residues. The experimental values of ^{1}H NMR chemical shifts were completely presented in Supplementary Material (Supplementary Tables S1 and S2). The presence of spreader signals of TOCSY spectrum acquired in the presence of SDS-d_{25} also indicated a well resolved structure, when compared to spectrum obtained in its absence (Fig. S1). Moreover, NOESY experiment performed without SDS-d_{25} showed few correlations and low intensities signals (Fig. S2B). The absence of inter-residual NOE correlations provided

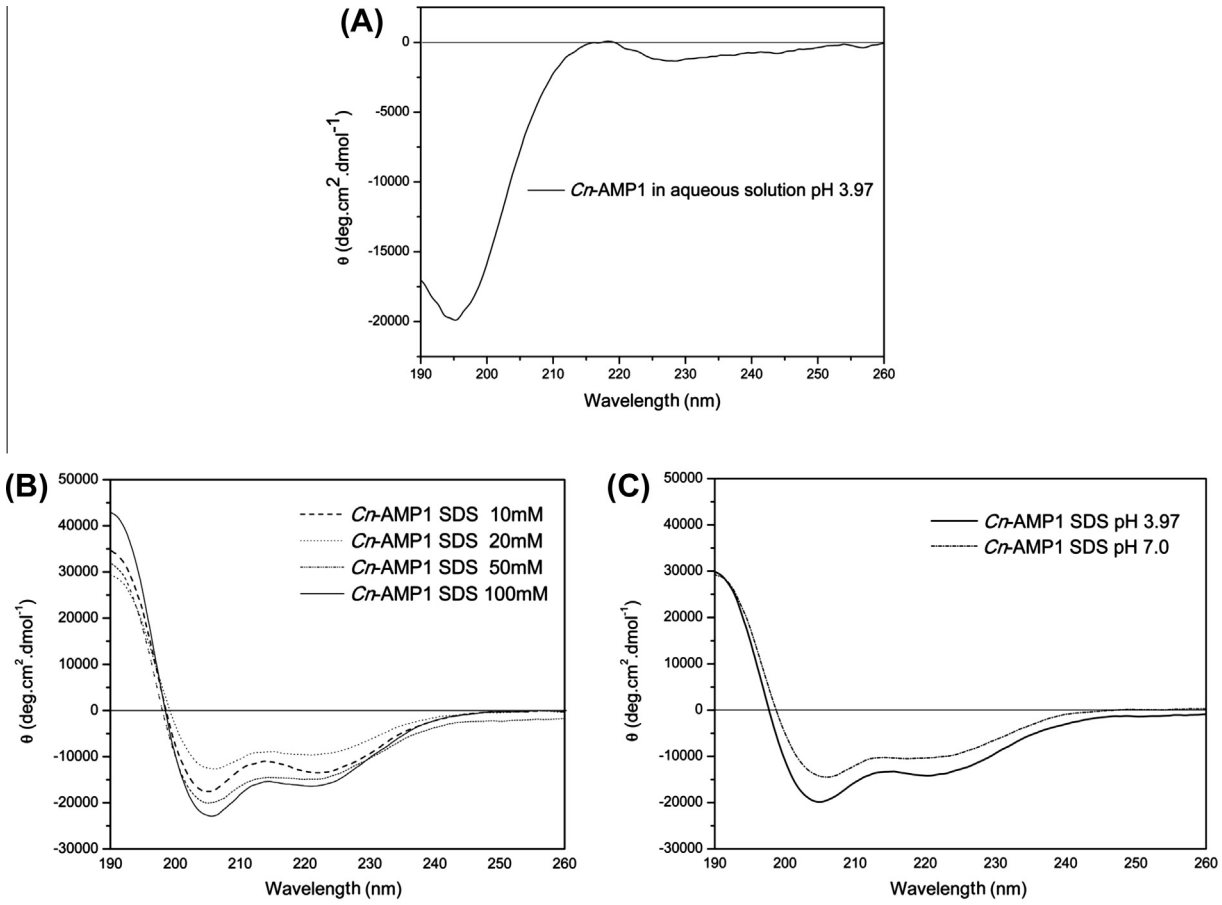

Fig. 1. CD spectra of 50 μM of *Cn*-AMP1 at 25 °C. (A) In aqueous solution (without SDS), (B) different concentration of SDS in water and (C) 100 mM of SDS at pH 3.97 (phosphate buffer) and pH 7.00 (Tris–HCl buffer).

again evidence that, in the absence of SDS-d_{25}, *Cn*-AMP1 shows a random conformation, as showed by CD spectrum for this condition. On the other hand, the NOESY experiment in SDS-d_{25} micelles presented well-resolved correlations and reliable intensity (Fig. S2A), which allowed dipolar coupled nucleus analyses.

Therefore, for the peptide in the presence of 100 mM of SDS-d_{25} at pH 3.97, the NOE correlations were properly identified and assigned in the NOESY map using the sequential assignment method [20]. The signals assignment of NOESY allowed us to construct the connectivity map H_N-H_α to *Cn*-AMP1 in the presence of 100 mM of SDS-d_{25}, as shown in S2A. The connectivity sequence of *Cn*-AMP1 residues in the above condition was confirmed when examining the region H_N-H_N (i, $i+1$) of inter-residual interactions. This region shows the connections between residues, thereby clearly confirming the *Cn*-AMP1 primary structure. The presence of correlations of type H_N-H_α and H_N-H_β ($i+3$ and $i+4$) of Ser-1 indicates an α-helical structure in this peptide portion when the peptide is in the presence of SDS micelles (Fig. S2A). The summary of NOE connectivity pattern is presented in Fig. 2. It is observed that the integral values of NOE $i-i+3$ and NH–NH are in the same order of magnitude, suggesting close spatial distances (Table S3). On the other hand, the interactions $i-i+3$ and NH–NH for 5HN–2HA and 9HN–8HN, show clear differences due to structural flexibility caused by ^{4}Gly and ^{8}Gly, respectively.

After complete assignment, the volume of the correlations from the NOESY contour map were converted into distance, and 118 distance restraints were obtained, with an average of 13.1 restrictions per residue, 43 of these being intraresiduals, 33 short-distance and 42 medium-distance (Table S4). The NOE connectivity diagram

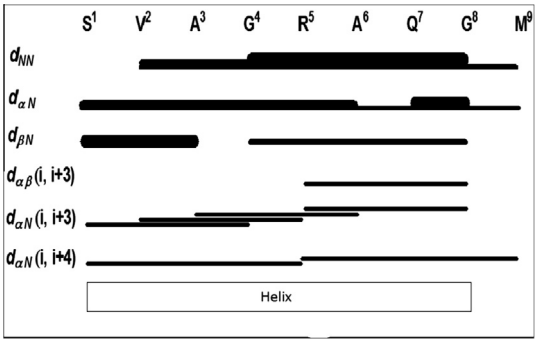

Fig. 2. Summary of the sequential and medium-range NOEs observed for the SDS-d_{25} micelles bound peptide *Cn*-AMP1. The thickness of the lines is proportional to the peak intensity.

(Fig. 2) also showed many medium distance restrictions of the type $d_{\alpha N}$ (i, $i+3$) between Ser-1/Gly-4, Val-2/Arg-5, Ala-3/Ala-6 and Arg-5/Gly-8 residues. The presence of these interactions suggests a structured segment with helical conformation between these residues. The two restrictions of $d_{\alpha N}$ (i, $i+4$) type, observed between Ser-1/Arg-5 and Arg-5/Met-9 residues, indicate a reliable structural ordering of the peptide. The non-observed H_N correlation of the Ser-1 residue suggests a kind of dynamic in this portion of the peptide, probably due to the liability of the amide hydrogens, exchanging rapidly with the solvent. However, the presence of $d_{\alpha N}$ (i, $i+3$ and i, $i+1$) restrictions indicates a helical structure of the peptide also in the N-terminal portion. Fig. S3 shows the distribution of the

main inter-residual interactions that contribute to peptide structuring.

For the representation of *Cn*-AMP1 structure in the presence of 100 mM of SDS-d_{25} at pH 3.97, 200 structures were generated and then the 20 lowest energy conformations were taken, thereby obtaining a family of conformations of the peptide. The structures were visualized using the program PyMOL [19]. Statistical data from these structures are listed in Table 1. H-bonds measured in the family of 20 models were also presented in Table S5.

A model of *Cn*-AMP1 which represents the peptide random structure in the absence of SDS-d_{25} micelles was presented in Fig. 3A since in water environment a coil structure is obtained for coconut peptide, as showed by CD and NMR data. Otherwise, Fig. 3B and C shows the superimposition of the 20 lowest energy structures for *Cn*-AMP1 in the presence of 100 mM of SDS-d_{25} at pH 3.97. The three-dimensional structure of *Cn*-AMP1 shows a helical structure between the Ser-1 and Ala-6 residues, which represents a helical content of 66.7%, a value previously predicted by in silico theoretical modeling [9]. H-bonds involving atoms between residues Arg-5-Ser-1; Arg5-Val-2 and Ala-6-Val-2 (Table S5) stabilize the secondary structure element and confirms the tendency of peptide to form an α-helical structure. However, due to conformational dynamics, the Ser-1 residue does not form an effective α-helix, although its interactions i, $i+3$ and i, $i+4$ might have reinforced this formation. The molecule has also no α-helical structure in the C-terminal portion between Gln-7 and Met-9 residues. The mobility related to the presence of Gly-8, associated with the proximity of two hydrophilic residues, Gln-7 and Gly-8, probably justifies the random conformation in this small part of the molecule. The absence of H-bond in residue Gln-7 and Gly-8, as showed in Table S5, also reinforce this result.

Random conformations in the absence of certain hydrophobic conditions like micelles or membranes have been observed before for other linear antimicrobial peptides. Indeed, data reported here corroborate the theoretical data presented for *Cn*-AMP1 by using molecular modeling [9,11]. Moreover, other AMPs also showed similar structural transitions. In the case of the multifunctional peptide Pa-MAP1 [21], derived from a polar fish, a conformational transition was detected in which a random fold in water was observed by circular dichroism spectral data and molecular dynamics. Nevertheless, in this same report a full α-helical core for this same peptide was observed in SDS and TFE environments. In summary, it seems that conditions could directly affect multifunctional and promiscuous peptides, as previously suggested by Franco [10], in a review that proposed that functions in fact are not only related to the primordial plant peptide structures but also to micro-environmental conditions that could drive the peptide fold. This idea was reinforced by the curiously parallel behavior observed here for other linear AMPs, including PGLa, a member of the magainin family [22], and LL37 [23], suggesting that their activity, especially at membrane levels, could be largely governed by micro-environmental properties, or in this case the constituent lipids [22]. Otherwise, selectivity against different cell types could be additionally run by an electrostatic attraction between the peptide and cellular surface. Interestingly, not only transitions between the random and helical structures have been observed. Some peptides may adopt, according to their primary structure and certain conditions, an α-helical structure able to disrupt DMPC and DMPG vesicles, in the case of non-selective peptides, or a β-sheet structure only capable of permeabilizing DMPG vesicles, in the case of selective peptides [24]. These data indicate that structural perturbation induced in selective peptides is much higher when compared to induction of non-selective peptides in the presence of lipids. This perturbation is associated with peptide aggregation due to higher concentrations and peptide orientation caused by the presence of lipids.

Table 1
Statistical data of the 20 lowest energy structures of the peptide *Cn*-AMP1.

Total distance restraints	118
Intra-residuals $\|i-j\|=0$	43
Short distance	33
Average distance ($2 \leqslant \|i-j\| \leqslant 5$)	42
Average restrictions per residue	13.1
RMSD (Å) all atoms	0.43 ± 0.16
RMSD (Å) α-helix	0.25 ± 0.19
Energy (kcal mol^{-1})	10.9
Residues in favored regions on Ramachandran diagram	95.1%
Residues in allowed regions on Ramachandran diagram	4.9%

The values of root mean square deviation (RMSD) calculated by the PyMOL software are clearly indicative of the enhanced conformational flexibility of peptide structure. These values are obtained by overlap of the 19 lowest energy structures, compared with the lowest energy structure. The RMSD values that are considered optimal for proteins are located in the range 1.0 <RMSD> 0.5, and can vary depending on the peptide [25]. Although the value calculated for the peptide under study is below the ideal (0.43 ± 0.16), the value here observed is representative, since the variation is within the expected error and also the RMSD tends to fluctuate with the molecule's dimensions. In such cases, larger compounds imply higher RMSD values. In this context, as the peptide under study has only nine residues in the chain, a lower value for this parameter is justified [26]. Furthermore, the quality of *Cn*-AMP1 structures was evaluated by analyzing the Ramachandran diagram that is part of the PROCHECK-NMR software [18,25]. The peptide has a consistent distribution in the Ramachandran diagram, with 95.1% of the residue being located in α-helix favorable regions and only 4.9% of residues located in a region of lower energy stability. It is important to note that only glycine residues, which are known to provide great flexibility to peptide structure due to their low steric hindrance, are located in this region. Thus, the Ramachandran diagram indicates a top structural quality obtained for the peptide *Cn*-AMP1 (Fig. S4).

The role of glycines in peptide flexibility was previously observed for other linear peptides. Clavanin, a peptide isolated from the tunicate *Styela clava* shows two glycines at positions 6 and 13. Both glycines might act as flexible pivots that enable the hydrophobic clavanin N-terminal to be inserted into the bacterial membrane bilayer [27]. Moreover, a glycine-rich antimicrobial peptide isolated from guava seeds also showed numerous glycines that improve flexibility and seem to be closely involved in bactericidal activity [28], suggesting that glycines from *Cn*-AMP1 could be important to antimicrobial function since they improve peptide flexibility.

Other structural features also seem to be important for antimicrobial activities, including the cationic surface and amphipathicity. In the latter, calculations for this *Cn*-AMP1 structure indicated a hydrophobic rate of 25%, given the relative hydrophobic moment. This moment defines the amphipathic peptide profile, which seems to be important for interaction with the cell surface, as previously described, together with other multiple factors that included aggregation and charges [29].

Finally and no less importantly, in order to evaluate the kinetics of exchange of the backbone H_N of each residue, the exchange NMR experiment (H/D) was performed by acquiring TOCSY correlation maps of 1 mM *Cn*-AMP1 in the presence of 100 mM of SDS-d_{25} and 550 μL of H_2O/D_2O (60:40) at pH 3.97 (Fig. 4). The correlations at δ 3.80, δ 3.86, δ 4.24 and δ 4.31 assigned to the H_α of Gly-4, Gly-8, Arg-5 and Met-9, respectively, were observed after 427 min. At the end of the experiment (732 min), low intensity correlations were observed in the chemical shift at δ 3.78, δ 4.12 and δ 4.34, which were attributed to the H_α of the Gly-4, Arg-5 and Met-9

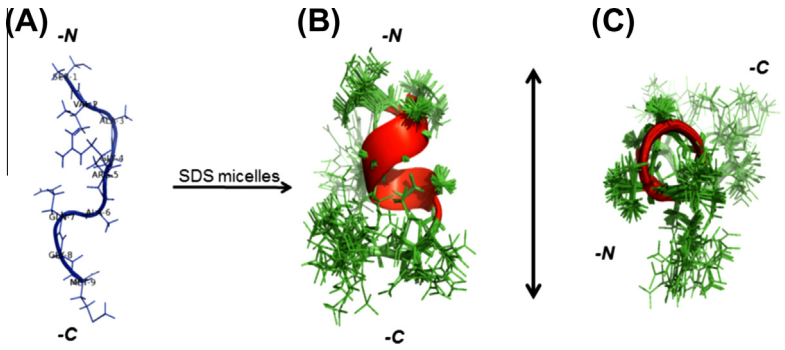

Fig. 3. (A) Model of *Cn*-AMP1 random structure (B); backbone overlap of the final 20 lowest-energy structures of 1 mM *Cn*-AMP1 peptide in presence of 100 mM SDS-d_{25} micelles, at 25 °C and pH 3.97. Helical formation is showed in ribbon, between Ser-1 and Ala-6 residues; (C) top view.

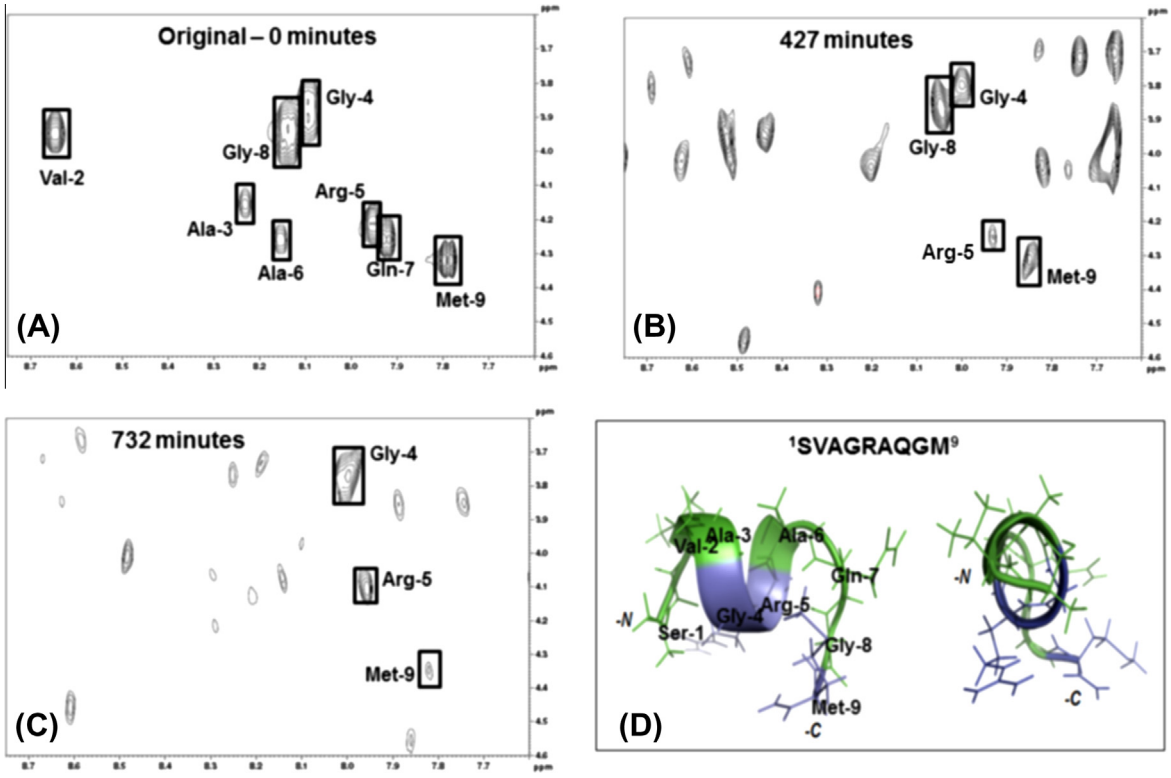

Fig. 4. Fingerprint region of TOCSY correlation map for 1 mM of *Cn*-AMP1 peptide in the presence of 100 mM SDS-d_{25}, at 25 °C and pH 3.97. (A) Original TOCSY, 90:10 (H_2O:D_2O); (B) exchange TOCSY H/D, 40:60 (H_2O:D_2O), after 427 min; (C) exchange TOCSY H/D, 40:60 (H_2O:D_2O), after 732 min. (D) Representation of the lowest energy structure of *Cn*-AMP1. The blue color shows the region of possible interaction with the cell membrane.

residues, respectively (Fig. 4). The NMR exchange experiment H/D showed that most of the H_N signals of the H_N-H_α correlation region, responsible for the peptide interaction with the cell membrane, disappeared and only those correlations assigned to Gly-4, Arg-5 and Met-9 were still present. This suggests a low solvent accessibility of these residues due to the interaction with the micelle. In the case of the Met-9 residue, which is not located in a helical region, the lower susceptibility to exchange suggests that this residue must lie immersed in the micelle, increasing the time required for such an exchange. The results of the exchange experiment and the presence of the positively charged residue (Arg-5) indicate that this is a possible interaction face with the cell membrane. Furthermore, Fig. 4D shows a possible *Cn*-AMP1 region that could show clear interactivity with negative surfaces, including bacterial membranes or nucleic acids, which are common targets for antimicrobial peptides [28].

Arginine residues are extremely important for a wide number of biological processes involving cell membranes. They are commonly found in antimicrobial and cell-penetrating peptides, which frequently contain a great number of cationic residues joined with hydrophobic residues across different structures [30,31]. It has been demonstrated that some antimicrobial peptide classes, such as human α-defensins [32] and plant γ-defensins [33], need arginines exposed on the peptide surface and their removal or substitution reduced bacterial killing activity. Moreover, although some reports have described the need for several arginines [33], *Cn*-AMP1 just shows a single Arg-5 exposed, which suggests that a single arginine is sufficient to start the antimicrobial activity process. This fact was corroborated by simulations performed by MacCallum et al. [34] that suggest that transfer of multiple arginine residues into the membrane bilayer core is non-additive. Therefore, the cost of making a water defect for the first arginine

is the foremost energy factor. Once this imperfection is formed, the price of relocating additional arginines is negligible and can even be negative, with only a single arginine needed to start and maintain the complete process.

4. Conclusions

In summary, CD and NMR analyses performed here showed the first structural elucidation of the disulfide-free multifunctional and promiscuous peptide from plant sources named *Cn*-AMP1. Data reported here showed that peptide structure is transitory and could be different according to the micro-environment. In this regard, *Cn*-AMP1 showed a coil in a water environment or an almost complete (66.7%) α-helical structure in the presence of SDS-d_{25} micelles at pH 3.97. Moreover, deuterium exchange experiments showed that the Gly-4, Arg-5 and Met-9 residues are less accessible to solvent, suggesting that flexibility and cationic charges presented by those residues may be essential for the development of *Cn*-AMP1 multiple activities. This information directly contributes to structural classification of plant peptides, providing novel insights into structure–functional relations in disulfide-free peptides. This, in turn, could be used to design novel and better peptides that could be biotechnologically applied to control bacterial infections and cancers.

Acknowledgements

The authors acknowledge the Coordenação de Aperfeiçoamento de Pessoal de Nível Superior (CAPES), the Conselho Nacional de Desenvolvimento Científico e Tecnológico (CNPq), Fundação de Amparo à Pesquisa do Estado de Goiás (FAPEG), Fundação de Apoio ao Desenvolvimento do Ensino, Ciência e Tecnologia (FUNDECT) and the Financiadora de Estudos e Projetos (FINEP) for their financial support.

Appendix A. Supplementary data

Supplementary data associated with this article can be found, in the online version, at http://dx.doi.org/10.1016/j.febslet.2015.01.029.

References

[1] Wu, G., Wu, H., Fan, X., Zhao, R., Li, X., Wang, S., Ma, Y., Shen, Z. and Xi, T. (2010) Selective toxicity of antimicrobial peptide S-thanatin on bacteria. Peptides 31, 1669–1673.
[2] Teixeira, L.D., Silva, O.N., Migliolo, L., Fensterseifer, I.C. and Franco, O.L. (2013) In vivo antimicrobial evaluation of an alanine-rich peptide derived from *Pleuronectes americanus*. Peptides 42, 144–148.
[3] de Oliveira Junior, N.G., e Silva Cardoso, M.H. and Franco, O.L. (2013) Snake venoms: attractive antimicrobial proteinaceous compounds for therapeutic purposes. Cell. Mol. Life Sci. 70 (24), 4645–4658.
[4] Roy, A., Mahata, D., Paul, D., Korpole, S., Franco, O.L. and Mandal, S.M. (2013) Purification, biochemical characterization and self-assembled structure of a fengycin-like antifungal peptide from *Bacillus thuringiensis* strain SM1. Front. Microbiol. 4, 332.
[5] de Souza Cândido, E., e Silva Cardoso, M.H., Sousa, D.A., Viana, J.C., de Oliveira-Júnior, N.G., Miranda, V. and Franco, O.L. (2014) The use of versatile plant antimicrobial peptides in agribusiness and human health. Peptides 55, 65–78.
[6] Tavares, L.S., Santos Mde, O., Viccini, L.F., Moreira, J.S., Miller, R.N., et al. (2008) Biotechnological potential of antimicrobial peptides from flowers. Peptides 29, 1842–1851.
[7] Pelegrini, P.B., Noronha, E.F., Muniz, M.A.R., Vasconcelos, I.M., Chiarello, M.D., Oliveira, J.T.A., et al. (2006) An antifungal peptide from passion fruit (*Passiflora edulis*) seeds with similarities to 2S albumin proteins. Biochem. Biophys. Acta 1764, 1141–1146.
[8] Pelegrini, P.B., Murad, A.M., Silva, L.P., dos Santos, R.C.P., Costa, F.T., Tagliari, P.D., et al. (2008) Identification of a novel storage glycine-rich peptide from guava (*Psidium guajava*) seeds with activity against Gram-negative bacteria. Peptides 29, 1271–1279.
[9] Mandal, S.M., Dey, S., Mandal, M., Sarkar, S., Maria-Neto, S. and Franco, O.L. (2009) Identification and structural insights of three novel antimicrobial peptides isolated from green coconut water. Peptides 30, 633–637.
[10] Franco, O.L. (2011) Peptide promiscuity: an evolutionary concept for plant defense. FEBS Lett. 585 (7), 995–1000.
[11] Silva, O.N., Porto, W.F., Migliolo, L., Mandal, S.M., Gomes, D.G., Holanda, H.H., Silva, R.S., Dias, S.C., Costa, M.P., Costa, C.R., Silva, M.R., Rezende, T.M. and Franco, O.L. (2012) Cn-AMP1: a new promiscuous peptide with potential for microbial infections treatment. Biopolymers 98 (4), 322–331.
[12] Chan, W.C. and White, P.D. (2000)Fmoc solid phase peptide synthesis: a practical approach, vol. 222, Oxford University Press, New York. pp. 1–376.
[13] Delaglio, F., Grzesiek, S., Vuister, G.W., Zhu, G., Pfeifer, J. and Bax, A.D. (1995) NMRPipe: a multidimensional spectral processing system based on UNIX pipes. J. Biomol. NMR 6 (3), 277–293.
[14] Johnson, B. and Blevins, R.A. (1994) NMRVIEW: a computer program for the visualization. J. Biomol. NMR 4, 603–614.
[15] Schwieters, C.D., Kuszewski, J.J. and Clore, G.M. (2006) Using Xplor-NIH for NMR molecular structure determination. Prog. NMR Spectrosc. 48, 47–62.
[16] Schwieters, C.D., Kuszewski, J.J., Tjandra, N. and Clore, G.M. (2003) The Xplor-NIH NMR molecular structure determination package. J. Magn. Reson. 160, 66–74.
[17] Hyberts, S.G., Goldberg, M.S., Havel, T.F. and Wagner, G. (1992) The solution structure of eglin C based on measurements of many NOEs and coupling constants and its comparison with X-ray structures. Protein Sci. 1, 736–751.
[18] Laskowski, R.A., Rulmann, J.A.C., Macarthur, M.W., Kaptein, R. and Thornton, J.M. (1996) AQUA and PROCHECK-NMR: programs for checking the quality of protein structures solved by NMR. J. Biomol. NMR 8 (4), 477–486.
[19] Delano, W.L. (2002) The PyMOL molecular graphic on world wide web http:s system, 2002 on World Wide Web http://www.pymol.org.
[20] Wüthrich, K. (1986) NMR of Proteins and Nucleic Acids, Wiley, New York.
[21] Migliolo, L., Silva, O.N., Silva, P.A., Costa, M.P., Costa, C.R., Nolasco, D.O., Barbosa, J.A., Silva, M.R., Bemquerer, M.P., Lima, L.M., Romanos, M.T., Freitas, S.M., Magalhães, B.S. and Franco, O.L. (2012) Structural and functional characterization of a multifunctional alanine-rich peptide analogue from *Pleuronectes americanus*. PLoS ONE 7 (10), e47047.
[22] Afonin, S., Glaser, R.W., Sachse, C., Salgado, J., Wadhwani, P. and Ulrich, A.S. (1838) 19F NMR screening of unrelated antimicrobial peptides shows that membrane interactions are largely governed by lipids. Biochim. Biophys. Acta 2014, 2260–2268.
[23] Wang, G., Mishra, B., Epand, R.F. and Epand, R.M. (1838) High-quality 3D structures shine light on antibacterial, anti-biofilm and antiviral activities of human cathelicidin LL-37 and its fragments. Biochim. Biophys. Acta 2014, 2160–2172.
[24] Fillion, M., Noël, M., Lorin, A., Voyer, N., Auger, M. (in press) Investigation of the mechanism of action of novel amphipathic peptides: insights from solid-state NMR studies of oriented lipid bilayers. Biochim. Biophys. Acta (http://dx.doi.org/10.1016/j.bbamem.2014.01.029).
[25] Lovell, S.C., Davis, I.W., Arendall III, W.B., Bakker, P.I.W., Word, J.M., Prisant, M.G., Richardson, J.S. and Richardson, D.C. (2002) Structure validation by Calpha geometry: phi, psi and Cbeta deviation. Protein Struct. Funct. Genet. 50, 437–450.
[26] Maiorov, V.N. and Crippen, G.M. (1994) Significance of root-mean-square deviation in comparing three-dimensional structures of globular proteins. J. Mol. Biol. 235, 625–634.
[27] van Kan, E.J., van der Bent, A., Demel, R.A. and de Kruijff, B. (2001) Membrane activity of the peptide antibiotic clavanin and the importance of its glycine residues. Biochemistry 40 (21), 6398–6405.
[28] Pelegrini, P.B., Murad, A.M., Silva, L.P., Dos Santos, R.C., Costa, F.T., Tagliari, P.D., Bloch Jr, C., Noronha, E.F., Miller, R.N. and Franco, O.L. (2008) Identification of a novel storage glycine-rich peptide from guava (*Psidium guajava*) seeds with activity against Gram-negative bacteria. Peptides 29 (8), 1271–1279.
[29] Fernandes, F.C., Rigden, D.J. and Franco, O.L. (2012) Prediction of antimicrobial peptides based on the adaptive neuro-fuzzy inference system application. Biopolymers 98 (4), 280–287.
[30] Mandal, S.M., Migliolo, L., Das, S., Mandal, M., Franco, O.L. and Hazra, T.K. (2012) Identification and characterization of a bactericidal and proapoptotic peptide from *Cycas revoluta* seeds with DNA binding properties. J. Cell. Biochem. 113 (1), 184–193.
[31] Epand, R.M. and Vogel, H.J. (1999) Diversity of antimicrobial peptides and their mechanisms of action. Biochim. Biophys. Acta 1462, 11–28.
[32] de Leeuw, E., Rajabi, M., Zou, G., Pazgier, M. and Lu, W. (2009) Selective arginines are important for the antibacterial activity and host cell interaction of human alpha-defensin 5. FEBS Lett. 583 (15), 2507–2512.
[33] Franco, O.L., Murad, A.M., Leite, J.R., Mendes, P.A., Prates, M.V. and Bloch Jr, C. (2006) Identification of a cowpea gamma-thionin with bactericidal activity. FEBS J. 273 (15), 3489–3497.
[34] MacCallum, J.L., Bennett, W.F. and Tieleman, D.P. (2011) Transfer of arginine into lipid bilayers is nonadditive. Biophys. J. 101 (1), 110–117.
[35] Tina, K.G., Bhadra, R. and Srinivasan, N. (2007) PIC: protein interactions calculator. Nucleic Acids Res. 35, W473–W476.